Population transfer by multiphoton adiabatic rapid passage

H. Maeda*
Department of Physics, University of Virginia, Charlottesville, Virginia 22904-0714, USA and PRESTO, Japan Science and Technology Agency (JST),Kawaguchi, Saitama 332-0012, Japan

J. H. Gurian† and T. F. Gallagher
Department of Physics, University of Virginia, Charlottesville, Virginia 22904-0714, USA
(Received 10 May 2010; revised manuscript received 1 February 2011; published 21 March 2011)

The population of atoms in Rydberg states is efficiently transferred with a change in principal quantum number n of up to ten via multiphoton adiabatic rapid passage through a single multiphoton resonance using a frequency-chirped microwave pulse. A quantum-mechanical picture of multiphoton adiabatic rapid passage in a one-dimensional atom using a Floquet approach provides a good description of most, but not all, of the observed phenomena.

DOI: 10.1103/PhysRevA.83.033416 PACS number(s): 32.80.Rm, 32.80.Qk

I. INTRODUCTION

Adiabatic rapid passage (ARP) is a very efficient and robust way of transferring population between states, and population transfer through a sequence of states separated by similar but not identical transition frequencies is particularly interesting. Examples are a sequence of $\Delta v = 1$ vibrational transitions in a molecule [1–3], a sequence of $\Delta m = 1$ transitions of Rydberg Stark states [4], and a sequence of $\Delta n = 1$ transitions of high n Rydberg states [5]. Here v is the vibrational quantum number of the molecule, and n, ℓ, and m are the principal, orbital angular momentum, and azimuthal angular momentum quantum numbers of the atom. Large changes in the quantum numbers in these three cases can be induced by a sequence of ARP's through single-photon resonances. In all of these cases, the frequency must be swept over the range spanned by the single-photon transitions of the sequence. Thus, transfer of Rydberg atoms from $n = 70$ to 80 requires a frequency sweep from 19 to 13 GHz, 40% of the center frequency, as shown by Fig. 1(a).

An alternative to a sequence of single-photon ARP's is a single multiphoton ARP (MARP). The possibility of MARP in vibrational transitions has been described by Oreg *et al.* [6]. The well-known counterintuitive pulse sequence can be thought of as a form of MARP [7]. Instead of sweeping the frequency, the levels are shifted by the time-varying ac Stark shifts from the two laser pulses. MARP has been used to make circular states by Cheng *et al.* [8], and we have reported its use in producing large changes in n [9]. Specifically, we reported changes in n of up to 10 using MARP. The principal attraction of MARP, as opposed to a sequence of single-photon ARP's, is shown in Fig. 1. Population transfer from $n = 70$ to 80 by a sequence of 10 single-photon ARP's requires a frequency chirp of 6 GHz, while a chirp of only ~300 MHz is required using MARP at the 10-photon resonance. A chirp that is 2% rather than 40% of the center frequency is required. Of course, a stronger driving field is required, but in many cases, especially laser applications, the field requirement is easily met, while a large frequency sweep presents a formidable barrier.

Here we present a more extensive set of data obtained using MARP in Li Rydberg states lying between $n = 70$ and 80, as shown in Fig. 1. These data have been analyzed to extract quantitative measures of the resolution and efficiency of the population transfer as well as the microwave fields required. In the sections that follow, we present a brief description of ARP that gives the requirements for ARP. We then describe the experimental approach and present our observations and their analysis.

II. ONE-DIMENSIONAL FLOQUET MODEL

A one-dimensional Floquet model provides a remarkably accurate picture of the behavior of a Rydberg atom in a linearly polarized microwave field, and, due to its simplicity, it provides useful insight into the requirements for MARP. We assume the energy levels to be hydrogenic, that is, the energy of the state of principal quantum number n is given by

$$W = -\frac{1}{2n^2}. \tag{1}$$

We use atomic units unless specified otherwise. We consider an atom in the field $\hat{z}E\cos\omega t$, with $\omega \approx 1/n^3$, and we only consider the strong $\Delta n = 1$ transition matrix elements, which are given by [10]

$$\langle n|z|n+1\rangle = 0.3n^2, \tag{2}$$

and we ignore all $\Delta n > 1$ matrix elements. It is a reasonable approximation since the $\Delta n > 1$ matrix elements are substantially smaller than the $\Delta n = 1$ matrix elements, and the $\Delta n > 1$ transitions are far off resonant. The Floquet energies are obtained by adding or subtracting an integral number of microwave photon energies ω from each atomic energy given in Eq. (1). Since we are only considering energy-level spacings near $\omega = 1/n^3$, we make the rotating-wave approximation and only consider one block of the Floquet Hamiltonian matrix. It is a tridiagonal matrix. The diagonal elements are the Floquet energies, and the Floquet energy of the state of principal

*Present address: Department of Phys. and Math., Aoyama Gakuin University, Fuchinobe, Sagamihara 252-5258, Japan.
†Present address: Laboratoire Aimé Cotton, CNRS, Université Paris-Sud, Bât. 505, 91405 Orsay, France.

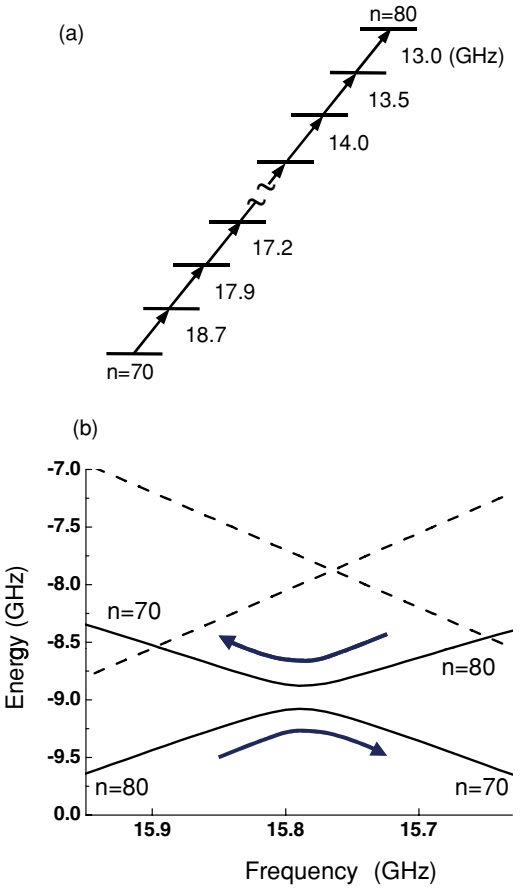

FIG. 1. (a) Energy levels for a sequence of ARP's of single-photon $\Delta n = 1$ transitions from $n = 70$ to 80. (b) Ten-photon avoided level crossing for a single ten-photon ARP from $n = 70$ to 80. The broken lines are the $n = 70$ and 80 Floquet levels in the absence of a microwave field, and the solid lines are the levels in the presence of a 3.7-V/cm microwave field. The avoided crossing may be traversed in either direction, as shown by the two arrows.

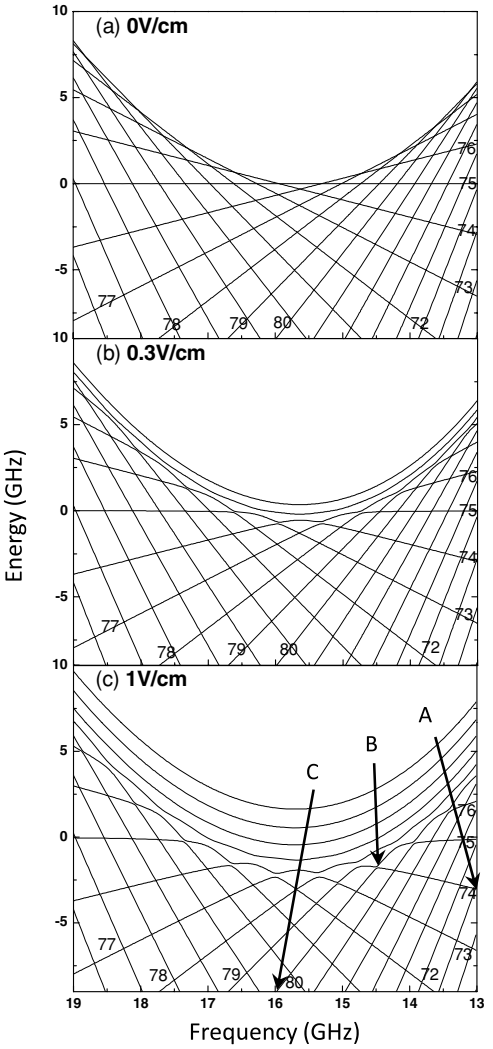

FIG. 2. (a) Floquet energy levels as defined in Eq. (1) for $60 \leqslant n \leqslant 90$ vs microwave frequency in zero microwave field. The $n = 72$–80 levels are labeled. The $\Delta n = 1$ resonances are the highest-lying level crossings, and $\Delta n > 1$ crossings are lower in energy. (b) With a microwave amplitude of 0.3 V/cm, the $\Delta n = k$, $k \leqslant 5$, and $k \leqslant 6$ avoided crossings become smooth curves in the higher and lower frequencies, respectively, the $\Delta n = 6$ avoided crossings are recognizable as isolated avoided-level crossings, and the $\Delta n \geqslant 7$ avoided crossings are invisible on this scale in the lower frequency region. (c) With a microwave amplitude of 1.0 V/cm, the $\Delta n = k$, $k \leqslant 5$, and $k \leqslant 6$ avoided crossings become smooth curves in the higher and lower frequencies, respectively, the $\Delta n = 6$ avoided crossings are recognizable as isolated avoided-level crossings, and the $\Delta n \geqslant 7$ avoided crossings are invisible on this scale in the lower frequency region.

quantum number n is given by

$$W_F = -\frac{1}{2n^2} - (n - 75)\omega. \tag{3}$$

In the microwave field $E \cos \omega t$, the off-diagonal matrix element b between states n and $n + 1$ is given by

$$b = 0.15n^2 E. \tag{4}$$

We choose the Floquet block in which the $n = 75$ state has no photons added because it is convenient for the graphical presentation of the Floquet energies.

In Fig. 2, we show plots of the Floquet energies versus microwave frequency $\nu = \omega/2\pi$ for several values of the microwave field strength. In Fig. 2(a), there is no microwave field, and the energies are straight lines. The $n = 75$ energy is a horizontal line, the $n > 75$ energies have positive slope, and the $n < 75$ energies have negative slope. At the $\Delta n = k$ resonances, where k is a positive integer, the levels cross since there is no coupling microwave field. The one-photon $\Delta n = 1$ resonances are at the top of the figure. The $\Delta n = 2$ resonances lie below the $\Delta n = 1$ resonances, but are offset in frequency. The $\Delta n = 3$ resonances, and all the Δn odd resonances, occur at frequencies similar to the $\Delta n = 1$ resonance. For example, the $n = 74$–75 resonance occurs at 15.95 GHz, the $n = 74$–76 resonance occurs at 15.65 GHz, and the $n = 73$–76 resonance occurs at 15.97 GHz.

In Fig. 2(b), we show the energy levels with a microwave field $E = 0.3$ V/cm, which produces a coupling matrix element $b = 324$ MHz at $n = 75$. This coupling leads to avoided crossings at all the resonances and is sufficiently strong that the avoided crossings at adjacent one-photon

$\Delta n = 1$ resonances overlap, leading to the smooth curve at the top of the figure. The same is true for the two-photon $\Delta n = 2$ resonances. The three- and four-photon couplings are, however, weak enough that there are well-resolved avoided crossings at these resonances. For the $\Delta n > 5$ resonances, the couplings are so weak that the avoided crossings are invisible on the scale of Fig. 2(b). In Fig. 2(c), we show the Floquet energies for $E = 1.0$ V/cm. At this microwave field strength, there are now four smooth curves at the top of the figure, corresponding to the overlapping avoided crossings of the $\Delta n = 1$ to 4 resonances. The avoided crossings at the $\Delta n = 5$ resonances are well resolved, and the avoided crossings at the $\Delta n > 5$ resonances are not visible. The coupling strengths of the avoided crossings decrease approximately a factor of 10 for each increase of Δn by 1. As shown by Figs. 2(b) and 2(c), the number of smooth curves, due to overlapping avoided crossings, increases with microwave field strength. The number of smooth curves is equal to the number of states that a nondispersing wave packet contains [11–13]. It is of interest to note that MARP can also be described in classical terms [14].

The strength of the $\Delta n = k$ coupling at the k photon resonance, Ω_k, is an important factor in determining whether ARP is possible. For the $\Delta n = 1$ one-photon resonances, the strength of the coupling is simply given by twice the off-diagonal matrix element,

$$\Omega_1 = 2b = 0.3n^2E. \tag{5}$$

The $\Delta n = k > 1$ coupling strengths can be calculated by perturbation theory or diagonalization of the Floquet Hamiltonian matrix, neither of which is particularly easy for $k > 2$. It is, however, straightforward to calculate the field at which adjacent $\Delta n = k$ avoided crossings begin to overlap to make the smooth curves of Fig. 2. The approximate requirement is that the $\Delta n = 1$ coupling must equal the maximum detuning. Since the $\Delta n = 1$ transition frequency is $1/n^3$, the maximum detuning of the $\Delta n = k$ transition is $3k/2n^4$. Equating this detuning to the $\Delta n = 1$ coupling of Eq. (2) leads to an approximate field requirement for the $\Delta n = k$ transition of

$$E_k = \frac{5k}{n^6}. \tag{6}$$

We expect ARP to occur at fields lower than that required to produce the smooth curves of Fig. 2, fields at which the avoided crossings are isolated, so Eq. (6) should be an upper limit to the field required. The probability P_k for ARP of an isolated $\Delta n = k$ avoided crossing on a linear sweep of the microwave frequency through the resonance is given by the Landau-Zener formula

$$P_k = 1 - \exp\left(-\frac{\pi^2{\Omega_k}^2}{kS}\right), \tag{7}$$

where Ω_k is the size of the avoided crossing in GHz, and the frequency sweep rate of the microwave field S is given in GHz/ns. The denominator of Eq. (7) is the rate at which the frequency separation of the levels of Fig. 2 changes, which is k times the sweep rate S, since the transition is a k photon transition. From Eq. (7), it is evident that the requirement for ARP of the $\Delta n = k$ resonance is approximately

$$\Omega_k > \frac{\sqrt{kS}}{\pi}. \tag{8}$$

The maximum sweep rate we can produce is 12 MHz/ns, and with this slew rate, Eqs. (5) and (8) imply that a microwave field of 0.02 V/cm is required for ARP of the $\Delta n = 1$ resonances at $n = 75$. Using Eq. (6) with the same slew rate implies that a field approaching 0.9 V/cm will be required for ARP of a $\Delta n = 6$ resonance.

ARP of a resonance requires that the frequency be swept through the avoided level crossing, and the minimum frequency sweep is given by

$$\Delta\nu = \frac{\Omega_k}{k}. \tag{9}$$

The required frequency sweep decreases as $1/k$, assuming that the adiabaticity requirement of Eq. (8) is met, which implies slower sweeps or higher fields for larger k. With our fastest slew rate, a sweep of 35 MHz is required for a $\Delta n = 1$ transition and a sweep of 14 MHz for a $\Delta n = 6$ transition. However, a field six times higher is required in the latter case.

III. EXPERIMENTAL METHOD

The experimental method is similar to that described in the previous paper [9]. Figure 3 is a schematic diagram of the experimental setup. Laser pulses from three dye lasers are used to excite Li atoms in a beam from the $2s$ ground state

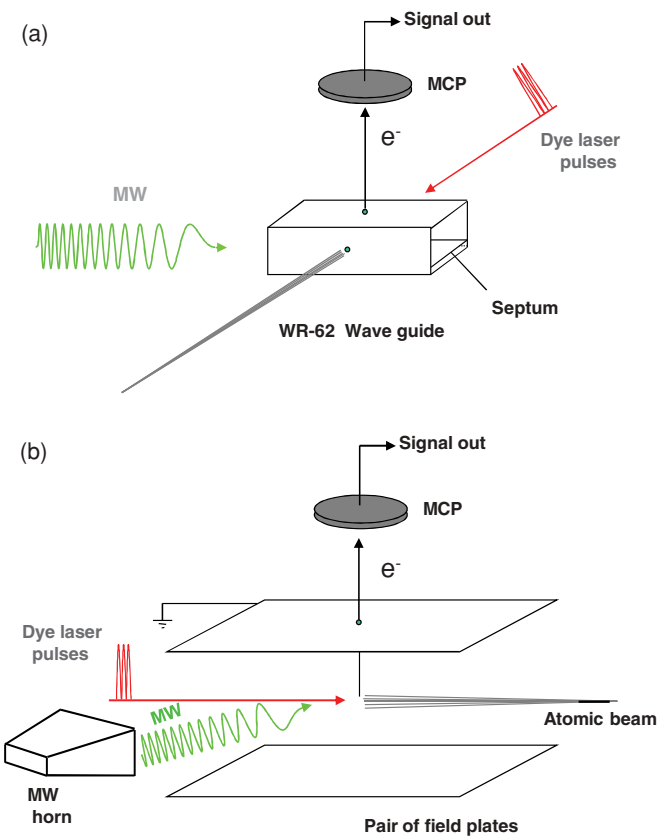

FIG. 3. (Color online) A schematic diagram of the experimental setup with (a) aWR-62 waveguide and (b) a pair of field plates.

to the np ($70 \leqslant n \leqslant 85$) Rydberg state via the $2p$ and $3s$ intermediate states. We use the second harmonic of a pulsed Nd : YAG laser with a 20-Hz repetition rate or a pulsed Nd : YLF laser with a 1-kHz repetition rate as a pump laser [15]. After exciting the atoms to the np state, we expose them to a chirped microwave pulse from a Siversima VO3260P/00 voltage-controlled oscillator (VCO). Interaction of the atoms with the laser pulses and a microwave pulse takes place in a piece of WR-62 waveguide that has small 1-mm-diam holes in both sidewalls for the passage of the atomic and laser beams, as shown in Fig. 3(a). To monitor the change in n of the final atomic state after interacting with the chirped microwave field, we use field ionization [16]. A negative voltage ramp, whose slew rate is changeable, is applied to the septum mounted in the waveguide [see Fig. 3(a)]. There is a 1-mm-diam hole in the top of the waveguide to allow the electrons produced by field ionization to be ejected from the waveguide and detected by a dual microchannel plate (MCP) detector above the waveguide. In some cases, laser excitation of the atoms occurs between a pair of parallel field plates, as shown in Fig. 3(b). In this case, we use a microwave horn located at the edge of the plates, and the field-ionization pulse is applied to the lower plate. A hole in the center of the upper plate allows field-ionized electrons to pass to the detector.

The chirped pulse from the VCO covers the 13–19-GHz range, and its 10-mW output power is amplified by a MITEQ MPN 4-02001800-23P amplifier or a Hughes 8020H traveling-wave tube amplifier to reach a maximum power from 300 mW up to a few W. The chirp is controlled by changing the 0–16 V control voltage of the VCO with a Hewlett-Packard pulse generator with a variable rise time. With the maximum chirp rate of 12 MHz/ns, the entire 6-GHz range can be covered in a 500-ns-long pulse, and we have used such 500-ns-long pulses to transfer atoms by a sequence of single-photon ARP's. In the experiments reported here, we have sliced pieces from the chirped pulse using a MITEQ DM0520LW1 double-balanced mixer and a gating pulse from an arbitrary waveform generator (AWG). We have most often used rectangular-shaped pulses from the AWG to make chirped microwave pulses with 10 ns rise and fall times. When the pulses are 50 ns, we cannot detect a difference between a rectangular pulse and a Gaussian-shaped pulse. Although we have used slower chirp rates as well, to obtain the data shown here we have used the maximum chirp rate. The amplitude of the microwave pulse is precisely controlled by a voltage-controlled attenuator. We monitor the microwave power using a diode detector. We estimate that we are able to determine the microwave field amplitude with an uncertainty of 15%.

IV. RESULTS AND DISCUSSION

We analyze the final-state distribution using field ionization, and we show in Fig. 4 the field-ionization signals obtained when Li atoms in np states of even n lying between $n = 72$ and 84 are exposed to a 1-μs-long field ramp in the absence of a microwave pulse. The signals from the odd n states are interspersed between the even n states shown in Fig. 4. While there is substantial overlap of the signals from adjacent n states, the leading edges of the signals are well resolved. To simplify

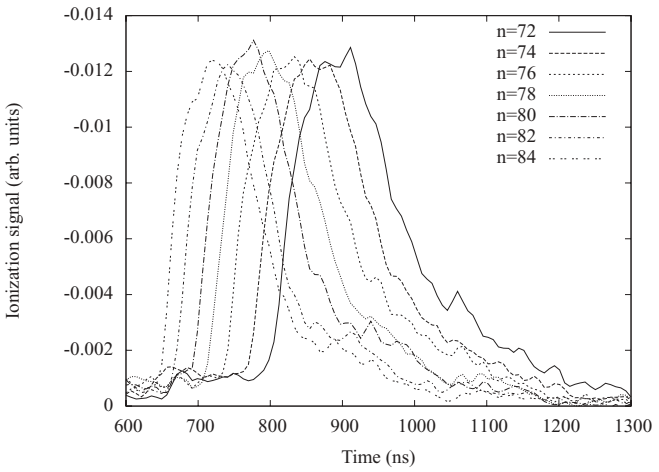

FIG. 4. Time-resolved field ionization signals of the even n, np states between $n = 72$ and 84. The odd n state signals are interspersed.

the discussion of subsequent figures containing time-resolved field-ionization signals, we convert the horizontal axis to n using the peak of the ionization signal for each n state. For example, $t = 778$ ns becomes $n = 80$.

Field-ionization traces such as those shown in Fig. 4 enable us to determine the final-state distribution when the atoms are ionized by the same field ramp subsequent to MARP. Figure 5 shows final-state distributions of Li atoms in the $74p$ state exposed to a 50-ns, 285-MHz positively chirped pulse. The data shown in each panel are gray-scale representations of time-resolved field-ionization electron signals for peak amplitudes of the microwave pulse ranging from less than 0.02 to 15 V/cm plotted against n. Panels (a)–(j) in this figure show the $\Delta n = +10$ to $+1$ transitions. For example, as shown in panel (a) of Fig. 5, the $n = 74$ to 84 transition occurs when atoms in $n = 74$ are exposed to a 50-ns, 285-MHz positive chirp pulse of $E \geqslant 2.1$ V/cm, whose center frequency is 13.57 GHz. As shown in Fig. 5, for small values of Δn the results are not sensitive to the field amplitude once the threshold field for MARP has been reached. For large values of Δn, there is only a small window of field strengths where MARP is possible without microwave ionization.

In Fig. 6(a), we plot the center frequencies of the multiphoton transitions with the positively chirped microwave pulse against Δn for initial states from $n = 71$ to 78, together with predicted frequencies of multiphoton transition as dotted curves. The frequencies are predicted from Eq. (1) and can also be extracted from the energy-level diagram of Fig. 2(a). The predictions do not include Stark shifts, which displace the resonances to higher frequency. In all cases, we started with the predicted center frequency and optimized the population transfer by a slight adjustment of the center frequency. For the initial state $n = 74$, the agreement between the experimental value and the predicted value is quite good, but there are slight discrepancies between experimental and predicted frequencies in other cases. We observe results essentially identical to those shown in Fig. 6 for 100-ns-long rectangular pulses with a 3 MHz/ns chirp rate.

It is useful to analyze the data shown in Fig. 5 in two ways. First, we can compare the fields at which MARP begins to occur to the fields computed using Eq. (6). For each panel

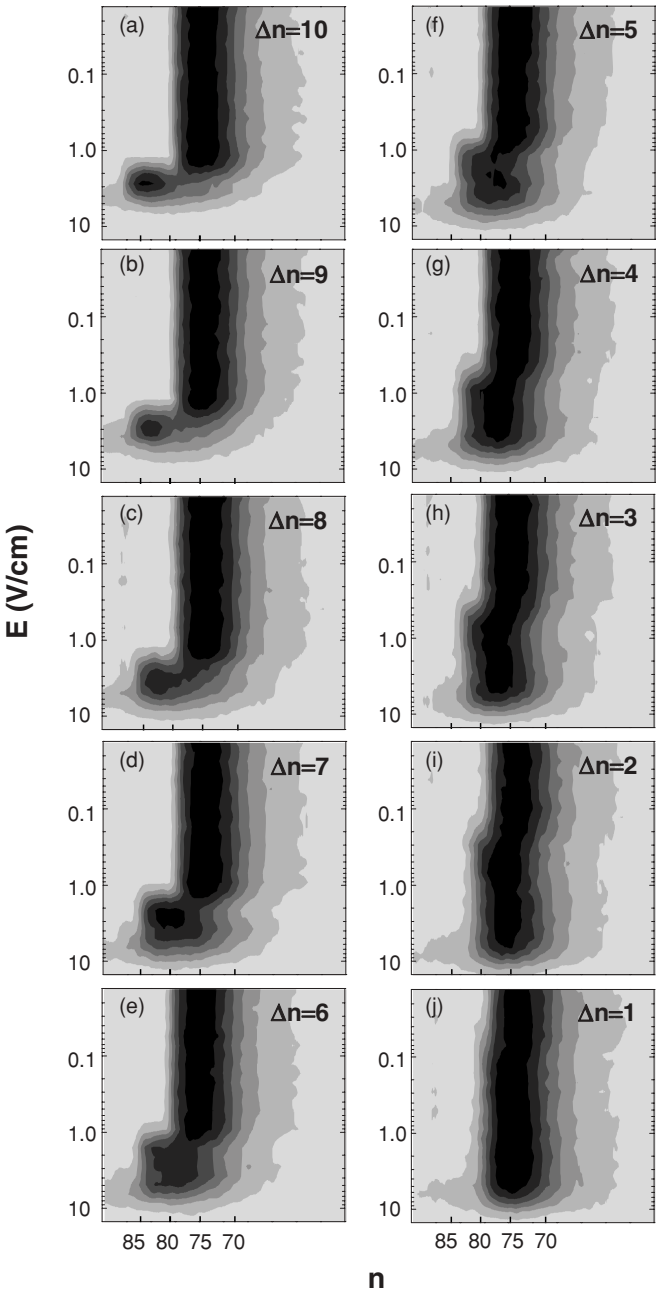

FIG. 5. Final-state distributions of $n = 74$ atoms exposed to a 50 ns, 285 MHz positively chirped pulse. Field strength of the microwave pulse is changed from less than 0.02 to 15 V/cm. Principal quantum numbers n of the initial and final states are defined experimentally using state-selective field ionization. Panels (a)–(j) show the $\Delta n = 10$–1 transitions.

of Fig. 5, we extract the $n = 74$ signal and the final n state signal as functions of the microwave field. As an example, in Fig. 7 we show the signals at $n = 74$ and 84 from Fig. 5(a) as a function of the microwave field amplitude. The rapid oscillations in the $n = 74$ signal at fields less than 2 V/cm are meaningless. It is apparent that there is a sharp increase in the $n = 84$ signal at $E = 3$ V/cm and a corresponding decrease in the $n = 74$ signal at the same field. The decrease in the $n = 74$ signal at $E = 3$ V/cm is not as sharp, in part due to the slowly falling tails of the field-ionization signals, as shown

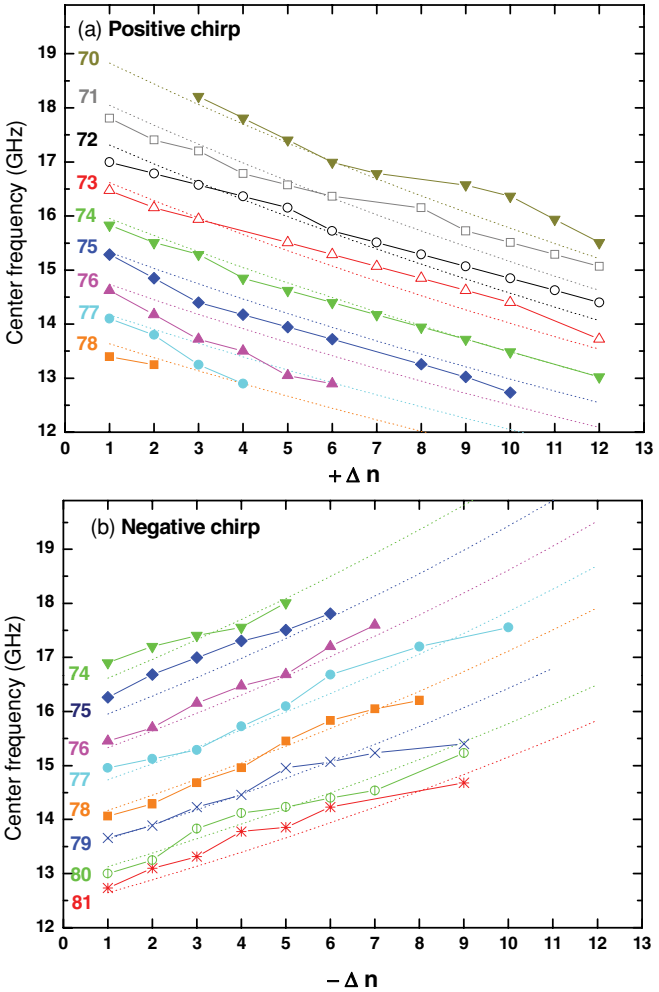

FIG. 6. (Color online) Plots of calculated and observed center frequencies of the 50-ns, 285-MHz chirped pulse for MARP of Li Rydberg atoms with (a) a positive chirp and (b) a negative chirp.

in Fig. 4. The $n = 84$ signal decreases at $E = 8$ V/cm due to the onset of microwave ionization. From plots analogous to Fig. 7, it is straightforward to determine the microwave fields at which the final-state signal reaches 50% of its maximum value, and we plot these fields versus $\Delta n = k$, the order of the multiphoton transition, in Fig. 8. The experimentally required fields are linear in $\Delta n = k$, as expected, but they lie above the prediction of Eq. (6) by almost a factor of 2.

Second, we can analyze the selectivity of MARP by fitting the field-ionization signals subsequent to MARP to a superposition of field-ionization signals from the n states between $n = 72$ and 84. This procedure is based on the assumption that the field-ionization signal for each n state shown in Fig. 4 is a good representation of the field-ionization signal for the same n state with a mixture of ℓ states produced by MARP. While it is not obvious that it should be, the assumption appears to be correct. Examining Fig. 5(j), which shows the $n = 74$ to 75 transition, we see that for fields less than 0.1 V/cm the signal is the same as the zero microwave field signal, and for fields greater than 0.1 V/cm the field-ionization signal is unchanged in shape, but shifted earlier in time to the location of the $n = 75$ signal.

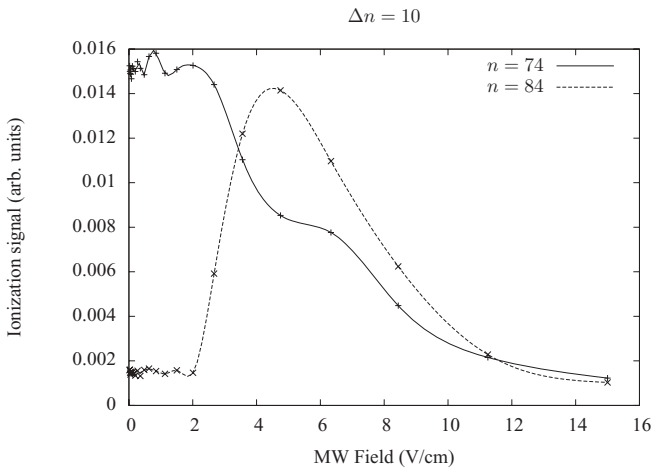

FIG. 7. The $n = 74$ and 84 signals from Fig. 5(a) vs microwave field. The oscillatory structure of the $n = 74$ signal at fields less than 2 V/cm is meaningless.

We fit the data by starting with an initial trial function that is a superposition of equal-amplitude field-ionization signals from $n = 72$ to 84. The fits to the final-state distributions of the $\Delta n = 4$, 7, and 10 MARP's are shown in Fig. 9 as well as the final-state histograms they yield. The final-state distributions consist of two components, atoms left in the initial $n = 74$ state and atoms transferred to higher-lying states. In Fig. 10, we show the final-state distributions for all the transitions of Fig. 5 in a gray-scale representation. Typically 30% of the atoms remain in the $n = 74$ state, and MARP results in the transfer of 70% of the population into two adjacent higher n states. However, in some cases more than 90% of the population transfer is to a single state, as shown by Fig. 10, but we do not understand what is special about these cases.

It is possible to observe population transfer to either higher or lower n states using MARP. In Fig. 11, we show final-state distributions of Li atoms initially in the $79p$ state exposed to a 50-ns, 285-MHz negatively chirped pulse. Panels (a)–(g) in this figure show the $\Delta n = -7$ to -1 transitions, respectively. We could not observe clear transitions from higher n to lower n when Δn is relatively large. Typically large fractional population transfer is only observed when Δn is less than 5. Presumably microwave ionization and $\Delta n > 1$ transitions compete with multiphoton population

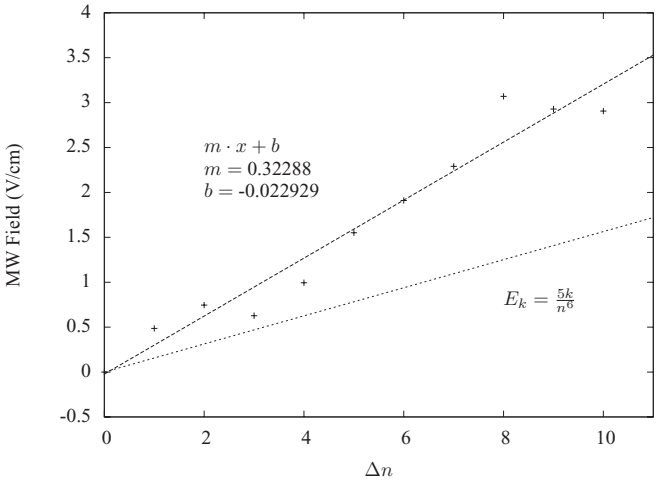

FIG. 8. Plot of the fields at which 50% of the maximum population transfer occurs vs Δn. The prediction of Eq. (6) is shown by the broken line.

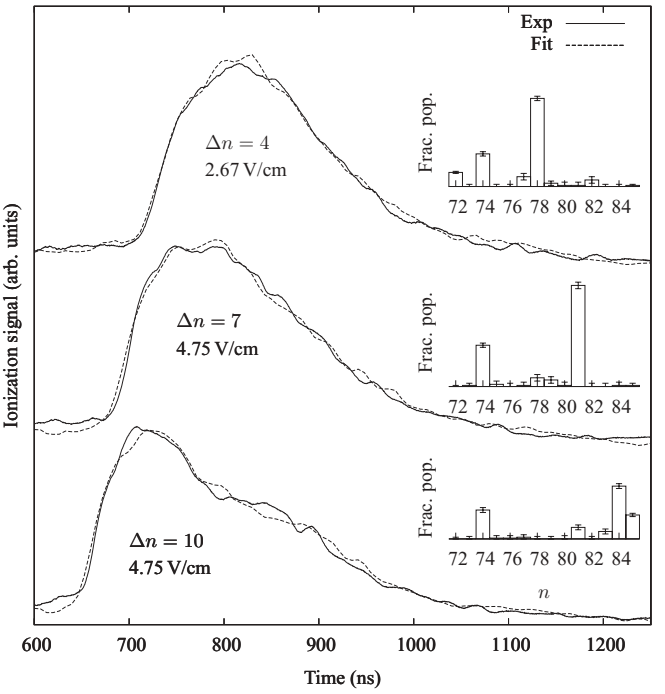

FIG. 9. Fits to the time-resolved ionization signals of the $\Delta n =$ 4,7, and 10 transitions of Fig. 5 to determine quantitatively the final-state distributions subsequent to MARP. The microwave field strengths are 2.67, 4.75, and 4.75 V/cm, respectively. The experimental data are plotted as solid curves and the fits as dashed curves. The rapid oscillations in both have no significance. Inset: histograms of the final-state distributions for each fit shown.

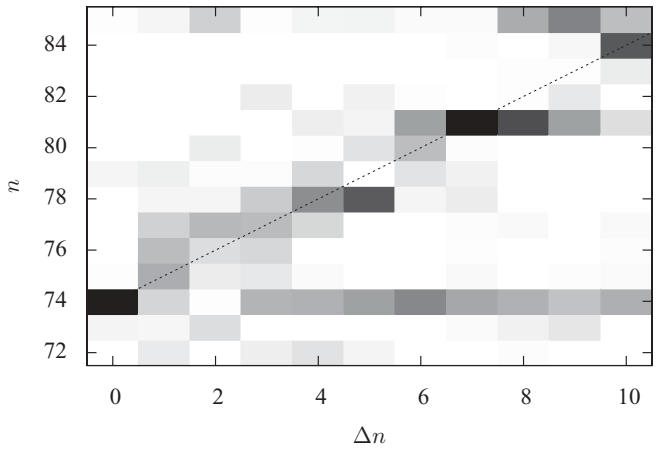

FIG. 10. Gray-scale rendering of the final-state distributions of the MARP transitions shown in Fig. 5. The initial state is in all cases $n = 74$, and the locus of the expected final state is shown by the dotted line. Typically 30% of the population remains in the $n = 74$ state, as shown by the obvious darkened bar at $n = 74$. Most of the population that is transferred to higher n states is typically found in two adjacent n states.

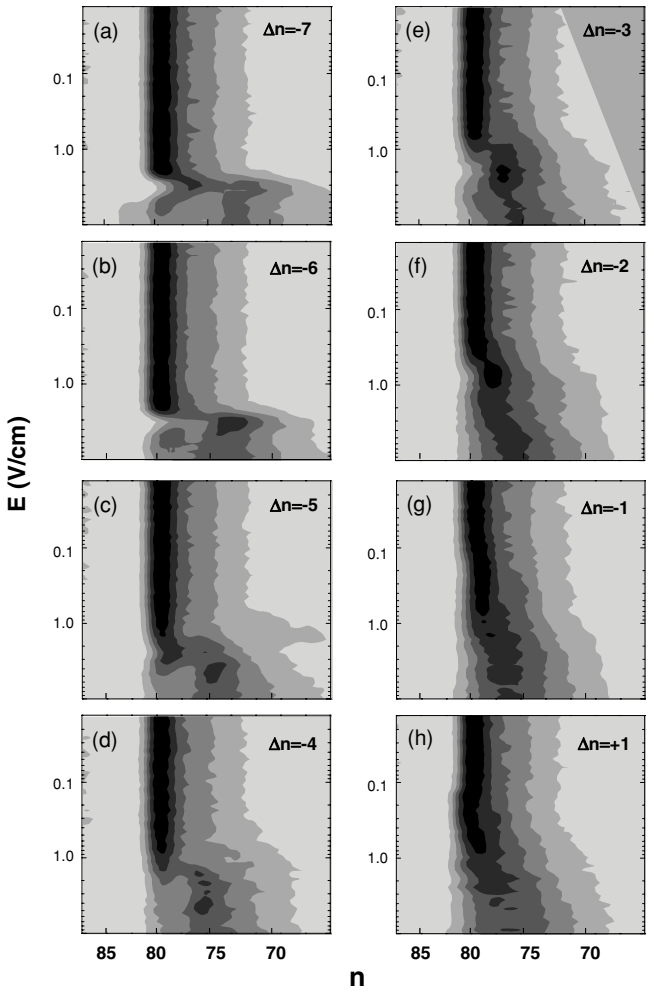

FIG. 11. Final-state distributions of $n = 79$ atoms exposed to a 50-ns, 285-MHz negatively chirped pulse. The field strength of the microwave pulse is changed from less than 0.02 to 10 V/cm. Principal quantum numbers n of the initial and final states are defined experimentally using the state-selective field-ionization method. Panels (a)–(g) show the $\Delta n = -7$ to $\Delta n = -1$ transitions. Panel (h) shows the $\Delta n = 1$ transition to $n = 80$.

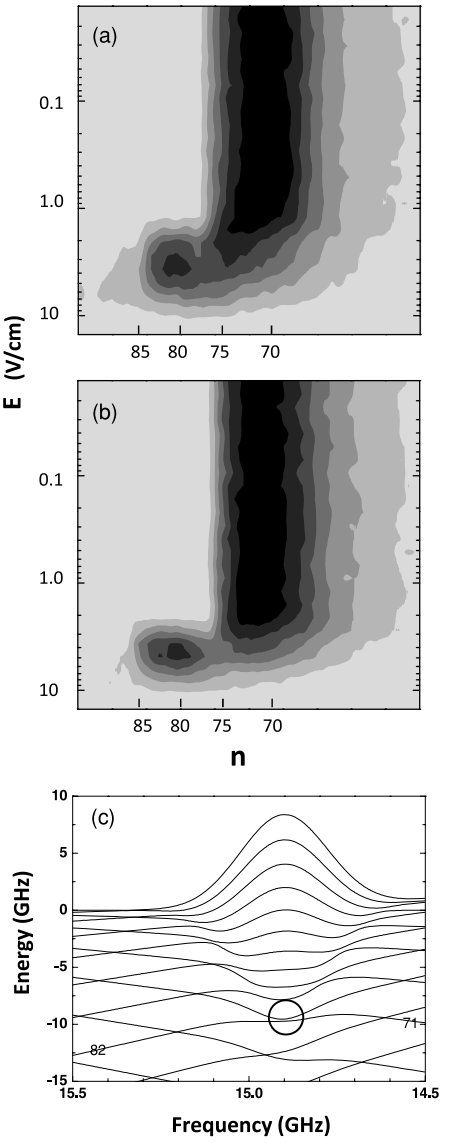

FIG. 12. Final-state distributions of $n = 71$ atoms exposed to a 50-ns, 285-MHz (a) negative chirp pulse and (b) positive chirp pulse. The field strength of the MW pulse is changed from less than 0.02 to 15 V/cm. Note that the center frequency measured in the experiment is slightly different from the calculated value. (c) Floquet energy levels of Rydberg atoms exposed to a 300-MHz chirped Gaussian pulse having the center frequency of 15.9 GHz with a peak field of 4 V/cm. Eleven-photon $n = 71$–82 avoided crossing at 14.9 GHz is circled.

transfer, suppressing the efficiency of higher n to lower n transitions, especially with the higher microwave intensity required to make larger Δn transitions. As shown in Fig. 6(b) the observed center frequencies of multiphoton transitions with the negatively chirped pulses agree well with the calculated transition frequencies.

Population transfer between two states should work equally well for frequency sweeps through a single or multiphoton resonance in either direction, as shown in Fig. 1. The insensitivity to the direction of the sweep for single-photon ARP is shown implicitly in Figs. 11(g) and 11(h), which show $\Delta n = +1$ and -1 transitions from $n = 79$, both observed with a negative chirp. The insensitivity to chirp direction is shown explicitly in Fig. 12, which shows the transitions from the $n = 71$ state to the $n = 82$ state with positive [Fig. 12(a)] and negative [Fig. 12(b)] chirped pulses. With both chirps we observe the same results. In Fig. 12(c), we show the Floquet energy levels for a chirped pulse with a Gaussian amplitude envelope. The energy levels are plotted versus frequency, and the peak amplitude occurs at 14.9 GHz (time runs to the left for a positive chirp and to the right for a negative chirp). While the levels do not look exactly like those shown in Fig. 2, the key point is that the energy ordering is preserved during the chirped pulse, which is why in Fig. 5 we observe the same population transfer once the threshold field is reached.

In conclusion, the results indicate that the fields required for MARP are in reasonable accord with the simple estimate of Eq. (6), i.e., that roughly 70% of the atoms undergo population transfer, and that the final-state uncertainty is ± 1 n state. The transfer probability of 70% is slightly less than the transfer probability of a sequence of single-photon ARP's, which was

estimated to be 80% for a $\Delta n = 10$ transition [5]. We attribute its being less than 100% to two factors. First, the atom is not a one-dimensional object. For each n state there are n $m = 0$ levels. Even if we confine our attention to $\Delta n = 1$ transitions, there are many different matrix elements. For example, the high ℓ $\Delta m = 0$ matrix elements are smaller than the $ns - (n+1)p$ $\Delta m = 0$ matrix elements. As a result, there exists a range of multiphoton coupling strengths. Second, the level structure of a Li atom is not hydrogenic. In a Li atom, the ns and np states have quantum defects of 0.30 and 0.05, respectively, so there is also a spread of allowed frequencies for each Δn transition, and the ac Stark shifts are very different.

The apparent width of the final-state distribution may be partially an artifact of the lack of resolution inherent in field ionization at this n level. It would be interesting to use resonance techniques as an alternative method of probing the final-state distribution. However, due to the sharp leading edges of the field-ionization signals shown in Fig. 4, we believe that more than one final n state is populated, which we attribute to the same factors that lead to less than 100% population transfer.

V. CONCLUSION

We have presented a quantitative analysis of multiphoton adiabatic rapid passage (MARP) in Rydberg states using chirped microwave pulses. The measurements show that it is possible to change the n state by up to 10 with comparable efficiencies, 70% to 80% using either a sequence of single-photon ARP's or MARP. The attraction of MARP is, of course, the substantial reduction in the chirp required, from 40% to 2% of the center frequency. Since the physics of this Rydberg problem and laser multiphoton transitions is very similar, we expect that MARP should be very attractive for laser manipulation of atoms and molecules.

ACKNOWLEDGMENTS

This work has been supported by the National Science Foundation under Grant No. PHY-0855572. H.M. has been supported by the JST PRESTO program. It is a pleasure to acknowledge useful discussions with D. V. L. Norum and F. Robicheaux.

[1] S. Chelkowski, A. D. Bandrauk, and P. B. Corkum, Phys. Rev. Lett. **65**, 2355 (1990).
[2] D. J. Maas *et al.*, Chem. Phys. Lett. **290**, 75 (1998).
[3] D. M. Villeneuve, S. A. Aseyev, P. Dietrich, M. Spanner, M. Y. Ivanov, and P. B. Corkum, Phys. Rev. Lett. **85**, 542 (2000).
[4] R. G. Hulet and D. Kleppner, Phys. Rev. Lett. **51**, 1430 (1983).
[5] H. Maeda, D. V. L. Norum, and T. F. Gallagher, Science **307**, 1757 (2005).
[6] J. Oreg, F. T. Hioe, and J. H. Eberly, Phys. Rev. A **29**, 690 (1984).
[7] N. V. Vitanov, T. Halfmann, B. W. Shore, and K. Bergmann, Annu. Rev. Phys. Chem. **52**, 763 (2001).
[8] C. H. Cheng, C. Y. Lee, and T. F. Gallagher, Phys. Rev. Lett. **73**, 3078 (1994).
[9] H. Maeda, J. H. Gurian, D. V. L. Norum, and T. F. Gallagher, Phys. Rev. Lett. **96**, 073002 (2006).
[10] R. V. Jensen, S. M. Susskind, and M. M. Sanders, Phys. Rep. **201**, 1 (1991).
[11] A. Buchleitner, D. Delande, and J. Zakrewski, Phys. Rep. **368**, 409 (2002).
[12] H. Maeda and T. F. Gallagher, Phys. Rev. Lett. **92**, 133004 (2004).
[13] H. Maeda and T. F. Gallagher, Phys. Rev. A **75**, 033410 (2007).
[14] T. Topçu and F. Robicheaux, J. Phys. B **42**, 044014 (2009).
[15] J. H. Gurian, H. Maeda, and T. F. Gallagher, Rev. Sci. Instrum. **81**, 073111 (2010).
[16] T. F. Gallagher, *Rydberg Atoms* (Cambridge University Press, Cambridge, 1994).